Geo-Mar Lett (2017) 37:537–547
DOI 10.1007/s00367-017-0506-6

ORIGINAL

Carbonate and silicate cementation of siliciclastic sediments of the New Jersey shelf (IODP Expedition 313): relation with organic matter diagenesis and submarine groundwater discharge

Catherine Pierre[1] · **Marie-Madeleine Blanc-Valleron**[2] · **Omar Boudouma**[3] · **Johanna Lofi**[4]

Received: 1 December 2016 / Accepted: 3 April 2017 / Published online: 8 April 2017

Abstract The New Jersey continental shelf extends 150 km off the shoreline. During IODP Expedition 313, siliciclastic deposits of late Eocene to late Pleistocene age were drilled down to 631, 669 and 755 m below seafloor at sites 27A, 28A and 29A respectively in very shallow waters (33.5 to 36 m depth). Pore water salinities display multilayered brackish-salty-brine units 10 to 170 m thick, where low-salinity water is preferentially stored in fine-grained sediments. The sharp boundaries of these buried aquifers are often marked by cemented layers a few centimetres thick. The mineralogy and scanning electron microscope observations of these layers show two phases of cementation by authigenic minerals: (1) the early carbonate cement is frequently associated with pyrite, and (2) the late silicate cement infills the residual porosity. The isotopic compositions of the carbonate cements vary widely: $-2.4 < \delta^{18}O$ ‰ VPDB $< +2.8$; $-15.1 < \delta^{13}C$ ‰ VPDB $< +15.6$. The $\delta^{18}O$ values indicate that the carbonate cements precipitated with pore waters comprising variable mixtures of seawater and ^{18}O-depleted fresh water originating from submarine groundwater discharge. The $\delta^{13}C$ values of the carbonate cements are related to organic matter diagenesis, providing ^{13}C-depleted dissolved inorganic carbon during bacterial sulphate reduction and anaerobic oxidation of methane, and ^{13}C-rich dissolved inorganic carbon during methanogenesis. The diagenetic cementation processes included chemical weathering of reactive silicate minerals by the CO_2-rich pore waters issued from organic matter diagenesis that released bicarbonate, cations and dissolved silica, which were further precipitated as carbonate and silicate cements. The estimated range of temperature (18±4 °C) during carbonate precipitation is consistent with carbonate cementation at moderate burial depths; however, silicate cementation occurred later during diagenesis at deeper burial depths.

✉ Catherine Pierre
catherine.pierre@locean-ipsl.upmc.fr

[1] UPMC-Sorbonne Universités, LOCEAN, 4 place Jussieu, 75252 Paris Cedex 05, France

[2] MNHN-Sorbonne Universités, CR2P, 57 rue Cuvier, 75005 Paris, France

[3] UPMC-Sorbonne Universités, ISTEP, 4 place Jussieu, 75252 Paris Cedex 05, France

[4] Geosciences Montpellier, Université Montpellier, 34095 Montpellier Cedex 5, France

Introduction

Many continental shelves around the world contain brackish water within the upper few hundreds of meters below the seafloor (Post et al. 2013). These subsurface low-salinity aquifers exist because of mixing between groundwater extending outwards and seawater diffusing from the overlying ocean. At some sites, the low-salinity offshore aquifers constitute vast meteoric groundwater reserves (VMGRs) with an estimated global volume of 3×10^5 km^3, which represents about one tenth of the global volume of shallow groundwater (Post et al. 2013).

The term "subterranean estuary" was proposed by Moore (1999) to describe these systems, where mixtures of fresh water and seawater would react with the sediment components of the aquifer and are released to the seafloor by submarine groundwater discharge (Burnett et al. 2003). This process is thought to have major impacts both on sediment diagenesis and on the biogeochemistry of the coastal ocean by providing nutrients and chemical elements from the discharging fluids.

The New Jersey continental shelf extends 150 km off the present-day shoreline and is considered by Post et al. (2013) as the best documented example of VMGRs. Indeed, it is a well-known area investigated by extensive drillings starting with the AMCOR (Atlantic Margin CORing) project (Hathaway et al. 1979) that discovered an extensive fresh-water aquifer within a few hundred meters below the seafloor. This finding was further documented by ODP drillings during Expedition 150 with four sites (902, 903, 904 and 906) on the New Jersey continental slope at water depths between 445 and 1,134 m (Mountain et al. 1994), Expedition 150X on the New Jersey coastal plain (Miller et al. 1994), and Expedition 174A on the New Jersey continental shelf and slope at three sites (1071, 1072, 1073) in 88 to 640 m water depth, where drilling recovered up to 664 m of sediment consisting of late-middle Miocene to Pleistocene sequences (Austin et al. 1998). At sites 1071 and 1072 on the outer continental shelf, the Cl and $\delta^{18}O$ profiles of pore waters covary and show two minima relative to average seawater that were interpreted by the mixing of seawater with about 20% of meteoric water (Malone et al. 2002). The late Miocene-Pliocene sedimentary sequence contains abundant nodules, layers and cemented pavements of authigenic carbonates. The carbonate mineralogy is dominated by siderite in the nodules and layers, whereas the pavements are cemented by dolomite and calcite (Malone et al. 2002). The oxygen and carbon isotopic compositions of these authigenic carbonates display large variations ($+1.3 < \delta^{18}O‰ < +6.5$; $-41.7 < \delta^{13}C‰ < +16.4$) that indicate carbonate precipitation with fluids of marine origin within the zones of sulphate reduction and methanogenesis (Malone et al. 2002).

During IODP Expedition 313 (April–June 2009), the siliciclastic deposits of late Eocene to late Pleistocene age forming clinoform wedges were drilled at the three sites M0027A, M0028A and M0029A (Fig. 1) down to 631, 669 and 755 mbsf (meter below seafloor) respectively in very shallow waters (33.5 to 36 m depth) on the upper continental shelf (Mountain et al. 2010; Table 1, Fig. 2). Examination of pore water samples from these sites reveals a large variation in salinity, such that chloride concentrations range between 41 and 994 mM (Fig. 3). The multilayered horizons of brackish to brine water are 10 to 170 m thick, and brackish water is stored preferentially in fine-grained sediments (Lofi et al. 2013; van Geldern et al. 2013). The $\delta^{18}O$-$\delta^{2}H$ and $\delta^{18}O$-Cl^{-} profiles show that pore waters from the subsurface down to 415 and 340 mbsf at sites M0027A and M0029A respectively

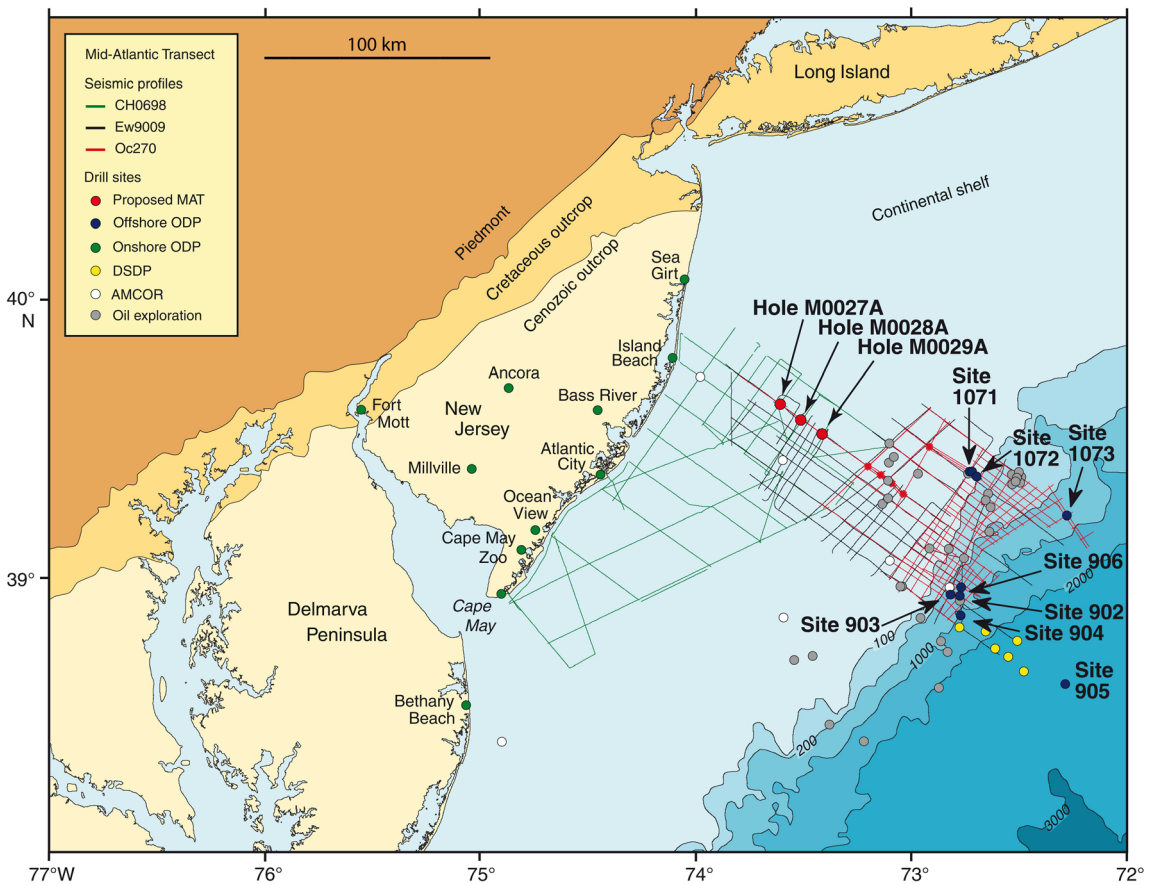

Fig. 1 Site map of Integrated Ocean Drilling Program Expedition 313 (IODP Exp. 313 New Jersey Shallow Shelf) and of other drilling sites (Ocean Drilling Program; AMCOR-Atlantic Margin Coring Project; extracted from Mountain et al. 2010)

Table 1 Coordinates, water depth (*mbsl* meter below sea level) and penetration (*mbsf* meter below seafloor) at drill sites M0027A, M0028A and M0029A during IODP Expedition 313 on the New Jersey shelf

Hole	Latitude	Longitude	Water depth (mbsl)	Penetration (mbsf)
M0027A	39°38.042067′N	73°37.301460′W	33.53	631.01
M0028A	39°33.942790′N	73°29.834810′W	35.05	668.66
M0029A	39°31.170500′N	73°24.792500′W	35.97	754.55

correspond to mixtures of seawater and meteoric water (Fig. 3). Downwards, the δ^{18}O-Cl^{-} profiles differ (Fig. 3) and indicate that there is a deep brine component mixed with meteoric water at site M0027A and with seawater at site M0029A (van Geldern et al. 2013). Authigenic carbonate nodules are present in the early to late Miocene sedimentary sequence at the three sites M0027A, M0028A and M0029A. Compared to the authigenic carbonates studied by Malone et al. (2002) that are located in the upper Miocene sediments, they have similar mineralogy (mostly siderite, ankerite, dolomite, calcite) but their oxygen and carbon isotopic compositions ($+0.4 < \delta^{18}O‰ < +4.8$; $-54.4 < \delta^{13}C‰ < +8.3$) are shifted to slightly lower values (van Geldern et al. 2013). Similarly to Malone et al. (2002), van Geldern et al. (2013) concluded that the authigenic carbonate nodules from the upper continental shelf were formed by fluids of marine origin with no contribution of meteoric water, in diagenetic zones where sulphate reduction and methanogenesis were active.

At the three sites M0027A, M0028A and M0029A, local lithified layers a few cm thick with very low permeability are located at the low salinity/saline water boundaries, and in the briny pore fluids for the lowermost cemented layers at site M0029A (Lofi et al. 2013). These layers have been studied for their physical properties (Lofi et al. 2013) but their mineralogy and isotopic composition of the carbonate cement have to date not been analyzed. The objective of the present mineralogical and stable isotope study was to characterize the diagenetic processes responsible for cementation within the siliciclastic deposits of the New Jersey shelf.

Geological setting

The New Jersey margin is a passive continental margin where the accumulation rate of siliciclastic sediment increased in the late Oligocene to Miocene, giving a thick pile of sediment wedges that built seawards and produced a terraced morphology with a shallow ramp and a deep ramp separated by a slope of 4–6° (Miller and Snyder 1997; Christie-Blick et al. 1998). At least 18 unconformably bounded sequences have been identified in the Miocene to Pleistocene succession of the New Jersey outer shelf (Christie-Blick et al. 1998), which are comparable to the early Oligocene to Pleistocene sequences bounded by 21 seismic reflectors in the succession of the New Jersey upper shelf (Inwood et al. 2013).

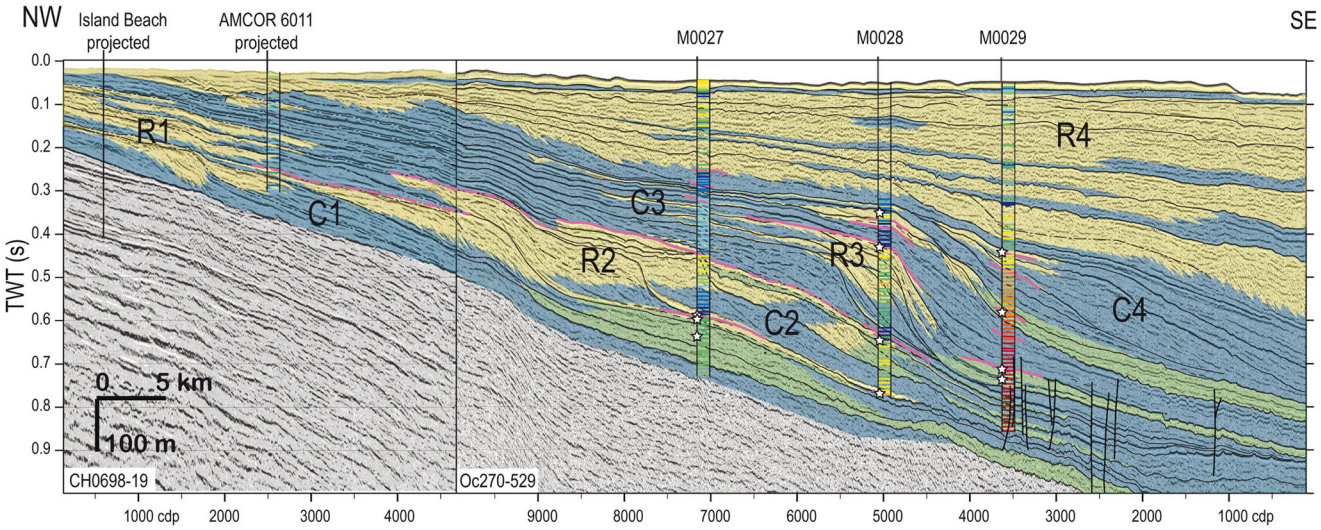

Fig. 2 Seismic profile along the New Jersey margin and location of the IODP 313 drilling sites (*TWT* two way travel time, *cdp* common depth point). The superimposed two-dimensional reservoir model shows the present-day architecture of the reservoirs (R1–R4) and the expected permeability (*yellow* high permeability, k>10^3 mD; *green* medium permeability, 10^{-1} < k < 10^3 mD; *blue* low permeability, k<10^{-1} mD). *Red contours* Cemented layers at low salinity/salt water boundaries. *Stars* Position of studied samples. (Figure modified from Lofi et al. 2013)

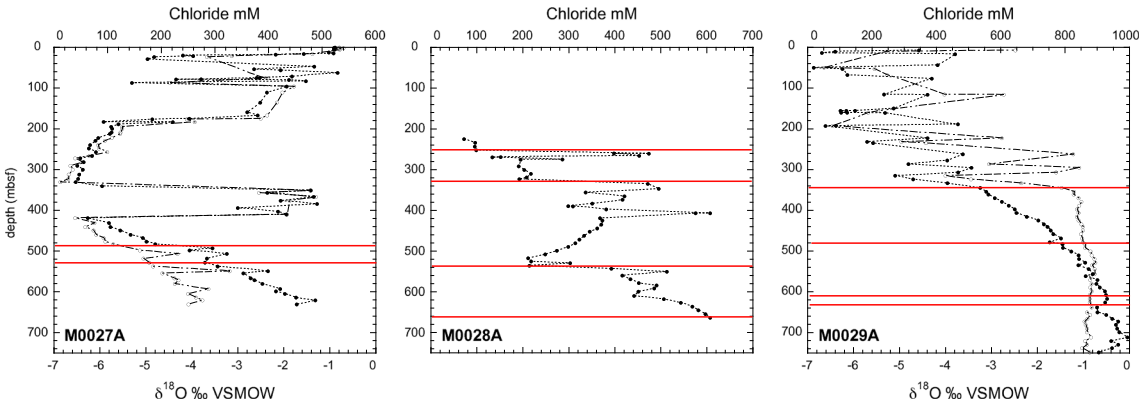

Fig. 3 Depth distribution of Cl^- concentrations (*filled circle*) and $\delta^{18}O$ values (*open circle*) in the pore fluids of IODP sites M0027A, M0028A and M0029A (data from van Geldern et al. 2013). *Horizontal red lines* Location of studied cemented layers

The three boreholes drilled during IODP Expedition 313 at sites M0027A, M0028A and M0029A are located at 45, 56 and 67 km respectively from the present-day shoreline (Fig. 1). Three main low-permeability fine-grained units containing low-salinity water and four permeable coarse-grained reservoirs containing salty water are superposed and interfingered, with very low-permeability cemented layers at the low salinity/salty water boundaries (Fig. 2; Lofi et al. 2013).

Materials and methods

Sediment sampling

A total of 11 samples of cemented layers lying between 254 and 664 mbsf were selected from the three sites M0027A, M0028A and M0029A of IODP Expedition 313 (Fig. 2, Table 2). These layers are located in the lower to middle Miocene sequences deposited during the interval between the seismic reflectors m6 and m4, dated at ~23.5 and ~13.5 Ma respectively (Mountain et al. 2010; Inwood et al. 2013). These samples were previously analyzed for porosity and permeability measurements by Lofi et al. (2013). The lithofacies of these cemented layers vary from coarse-grained sandstone that is generally glauconite-rich, to light beige/medium grey siltstone and claystone (Fig. 4). From each sample, a small fragment (about 1 g) was collected and grounded with an agate mortar to obtain a homogeneous powder used for further mineralogical and isotopic studies of the bulk sample. Moreover, observations under a binocular microscope identified fine carbonate veins and void fillings in the cement of six samples that was recovered with a dental drill before proceeding to isotopic analyses.

Mineralogy

The mineralogy of the cemented sedimentary layers allowed identifying the authigenic minerals present in the cement. The total carbonate content of sediment (weight % of dry sediment, wt%) was obtained with a manual calcimeter by digesting 100 mg of the bulk powder with 1 ml of an 8N HCl solution. X-ray diffraction (XRD) was systematically applied for the identification of minerals from all samples; non-oriented powder was analyzed using a diffractometer Brüker D2 Phaser equipped with a Lynxeye detector Cu-Kα radiation (λ=0.15406 Å) and Ni filter at 30 kV and 10 mA. Scanning electron microscope (SEM) observations coupled with chemical element analyses by dispersive energy X-ray spectrometer were made on all samples to characterize the crystal morphology and the chemical composition of the authigenic carbonates, and to identify other possible authigenic minerals.

Oxygen and carbon stable isotopes

The oxygen and carbon isotopic compositions ($\delta^{18}O$ and $\delta^{13}C$) of the carbonate fraction were determined on the bulk powdered sample and cement micro-samples. They served to characterize the nature of the fluids (water, dissolved inorganic carbon DIC) and to estimate the possible range of temperature from which the diagenetic carbonates precipitated. The conventional δ value corresponds to the relative difference in parts per mil (‰) between the isotopic ratio R ($^{18}O/^{16}O$, $^{13}C/^{12}C$) of the sample (s) and of the reference (r) VPDB (Vienna Peedee Belemnite) defined by Craig (1957) and revised by Gonfiantini et al. (1995):

$$\delta = [(Rs/Rr) - 1] \times 1,000$$

For the bulk powdered samples, the isotopic measurements were performed on the CO_2 produced offline at 25 °C from 100 to 500 mg of the sample (depending on the carbonate wt%) reacted with 100% orthophosphoric acid. The analyses were conducted on a dual inlet isotopic ratio mass spectrometer (DI-IRMS) VG-SIRA9. For the cement micro-sample, about 100 µg was reacted at 90 °C with orthophosphoric acid using the multicarb system coupled with a DI-IRMS VG-

Table 2 Sedimentary description, mineralogy, oxygen and carbon isotopic compositions of carbonate cements of lithified layers sampled at sites M0027A, M0028A and M0029A. *Bold* Dominant mineral in carbonate mixtures

Sample	Depth (mbsf)	Macrofacies	Carbonate mineralogy	Carbonate wt%	d (104) carbonate (Å)	Other minerals	$\delta^{18}O$ ‰ VPDB (micro-sample)	$\delta^{13}C$ ‰ VPDB (micro-sample)	$\delta^{18}O$ ‰ VPDB (bulk carbonate)	$\delta^{13}C$ ‰ VPDB (bulk carbonate)
M0027A										
313-27A-171-1, 38–39 cm	489.7	Sandstone, coarse-grained green (glauconite grains)	Siderite	7	2.794	Quartz, opal-CT, feldspars, glauconite, pyrite, gypsum	+2.8	+7.6	+2.6	+5.2
313-27A-174-1, 75–76 cm	494.5	Sandstone, coarse-grained green (glauconite grains)	Siderite	1	2.798	Quartz, opal-CT, feldspars, glauconite	+1.8	+4.5		
313-27A-190R-1, 31–33 cm	533.7	Sandstone, coarse-grained grey-green (glauconite grains)	Low-Mg calcite	21	3.026	Quartz, feldspars, glauconite, gypsum, zeolite, pyrite, goethite			−2.4	−10.4
M0028A										
313-28A-12R-1, 18–20 cm	254.0	Claystone, fine-grained beige-grey		0		Quartz, kaolinite, illite, feldspars, jarosite, gypsum, pyrite				
313-28A-40-1, 76–80 cm	327.6	Sandstone, coarse-grained green (glauconite grains)	Mg-siderite	16	2.805	Quartz, glauconite, pyrite, gypsum	+2.1	−9.4	+0.9	−9.3
313-28A-123-1, 67–69 cm	540.0	Sandstone, coarse-grained green (glauconite grains)	**Fe-dolomite** + siderite	37	2.901 (dol) 2.793 (sid)	Quartz, opal-CT, feldspars, glauconite, pyrite, gypsum	−0.4	−12.3	+0.4	−13.5
313-28A-169R-2, 14–15 cm	664.0	Sandstone, medium-grained brown	Low-Mg calcite	2	3.036	Quartz, feldspars, kaolinite, illite, glauconite, gypsum, pyrite, zeolite				
M0029A										
313-29A-72-1, 26–28 cm	343.6	Siltstone, fine-grained grey	Dolomite	76	2.888	Quartz, feldspars, illite/muscovite, kaolinite, pyrite	+1.6	−0.5	+1.3	−1.5
313-29A-119-1, 2–4 cm	479.5	Siltstone, fine-grained grey	**Dolomite** + siderite	76	2.898	Quartz, feldspars, illite/muscovite, kaolinite, pyrite	+2.4	+15.6	+1.5	+14.8
313-29A-164R-2, 86–88 cm	611.9	Sandstone, coarse-grained grey (glauconite grains)	**Low-Mg calcite** + ankerite	34	3.024	Quartz, opal-CT, feldspars, illite/muscovite, kaolinite, pyrite, amphibole			−2.4	−15.1
313-29A-173R-1, 100–101 cm	636.2	Sandstone, coarse-grained green (glauconite grains)	Siderite	1	2.798	Quartz, opal-CT, feldspars, glauconite, gypsum, pyrite, jarosite				

Fig. 4 Lithofacies (sandstone, claystone, siltstone) of three selected lithified layers from sites M0027A, M0028A and M0029A

Isoprime. For both mass spectrometers, the analytical precision 2σ is 0.01‰ and the reproducibility is ±0.05% for both $\delta^{18}O$ and $\delta^{13}C$ values.

Results

Petrography and mineralogy

The total carbonate content of the powdered sediment samples ranges from 1 to 76 wt%. The highest values were measured in site M0029A samples and the lowest values at all three sites (Table 2).

The bulk mineralogy of the cemented layers deduced from the XRD analyses (Table 2) corresponds to variable mixtures of minerals from the matrix and the cement. The siliciclastic matrix is composed of quartz (dominant), feldspars and clay minerals with more or less abundant glauconite. The authigenic minerals of the cement comprise carbonates (mostly dolomite and ankerite/siderite, low-Mg calcite generally in trace amounts), opal-CT, zeolite, pyrite, gypsum and jarosite. The opal-CT is present in the cemented layers deeper than 490 mbsf (Table 2).

The different authigenic minerals from the cements of the lithified layers are well identified by SEM observations (Figs. 5 and 6): *carbonates* [massive calcite cement is made of interconnected rhombs, often corroded (Fig. 5a); massive dolomite cement is also made of interconnected rhombs (Fig. 5b); ankerite/siderite occurs generally as isolated and clusters of rhombic or lens-shaped crystals (Fig. 5c, d)]; *silicates* [opal-CT is present as fine-grained coating, and micron-sized globules and lepispheres made of interconnected platy crystals, similar to the structures described by Flörke et al. (1976) and Kastner (1979; Figs. 5d and 6a, b); authigenic Fe-K-rich clay minerals (illite and glauconite) are present as rosettes of lamellar elements (Fig. 6b) that appear locally as the product of alteration of K-feldspars; clinoptilolite (zeolite) makes clusters of euhedral crystals]; *sulphide and sulphate minerals* [pyrite occurs as dispersed isolated grains and framboids that may be more or less oxidized (Fig. 5b); gypsum occurs as secondary euhedral crystals covering the detrital grains (Fig. 6c) or included in the cement; jarosite is locally present in small nodules where the platy crystals are associated with opal-CT (Fig. 6d)].

O and C isotopic compositions of authigenic carbonates

The oxygen and carbon isotopic compositions of authigenic carbonate from the bulk powdered samples and cement micro-samples of the cemented layers vary significantly: $-2.4 < \delta^{18}O$ ‰ VPDB $< +2.8$; $-15.1 < \delta^{13}C$ ‰ VPDB $< +15.6$ (Table 2, Fig. 7). The lowest $\delta^{18}O$ values occur in calcite cements (−2.4‰); dolomite and siderite cements exhibit low to relatively high $\delta^{18}O$ values (−0.4‰ to +2.8‰). Negative $\delta^{13}C$ values characterize calcite cements (−15.1‰ to −10.5‰), whereas dolomite and siderite cements are characterized by either negative or positive $\delta^{13}C$ values (−13.5‰ to +15.6‰).

Discussion

Water–rock interactions and mineral diagenesis

The diagenetic minerals of cements are the products of geochemical reactions between the sedimentary matrix and pore solutions. Paragenetic sequences would thus provide information on the different pathways responsible for diagenetic mineral precipitation during cementation. At sites M0027A, M0028A and below ~300 mbsf at site M0029A, pore fluids

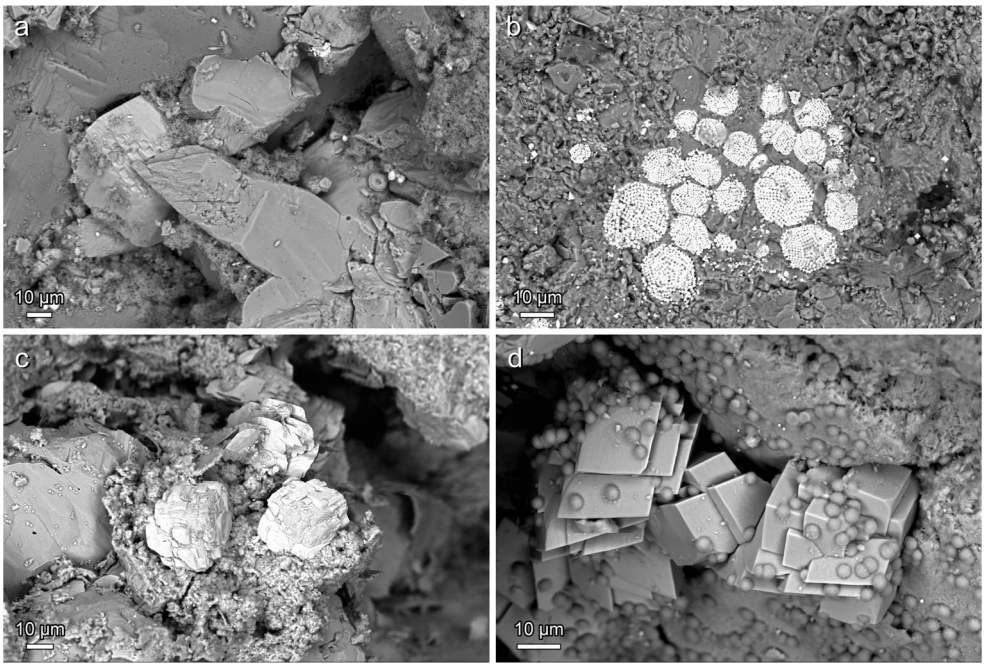

Fig. 5 SEM photographs of lithified layers from the IODP 313 drilling sites. **a** Sample 313-29A-164R-2, 86–88 cm: calcite cement with partial dissolution of crystals, one rhomb of ankerite, framboids of pyrite and coating by microspheres of silica. **b** Sample 313-29A-72-1, 26–28 cm: massive dolomite cement and framboids of pyrite. **c** Sample 313-28A-40-1, 76–80 cm: composite rhombs of Mg-siderite surrounded by fibrous silica cement. **d** Sample 313-27A-171-1, 38–39 cm: siderite rhombs covered with silica globules and cemented by fibrous silica

are characterized by high alkalinities (up to 29 mM) combined with high methane concentrations (up to 20,000 ppm) below ~200 mbsf (Mountain et al. 2010; van Geldern et al. 2013). At all sites, pore fluids also show marked variations in the concentrations of many elements (Ca, Mg, K, Fe, Ba, SO_4, Si), which indicate sources and sinks of these elements during mineral diagenesis (Mountain et al. 2010). The sulphur isotopic composition of sulphate of the pore fluids at site M0027A ($+20.0 < \delta^{34}S$ ‰ VCDT $< +27.4$) clearly indicates the marine origin of sulphate with a probable mixing in the briny fluids with sulphate from dissolved Jurassic evaporites, and the superimposition of bacterial sulphate reduction causing ^{34}S enrichment in the residual sulphate (van Geldern et al. 2013).

The SEM observations show that there are two major phases of cementation by authigenic carbonate and silicate minerals: (1) the early carbonate cement is made of Fe-dolomite, ankerite/siderite and occasionally calcite; pyrite was also precipitated during this phase, which was thus characterized by anoxic conditions; (2) the late silicate cement is made of opal-CT, Fe-K-rich clay minerals and zeolites filling in the residual porosity;

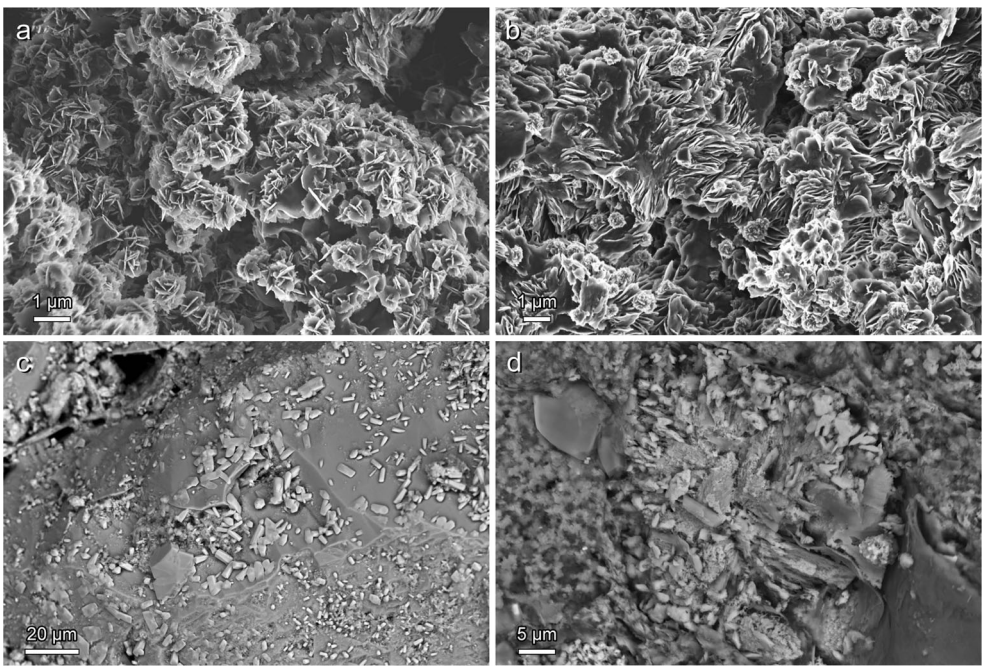

Fig. 6 SEM photographs of lithified layers from the IODP 313 drilling sites. **a** Sample 313-29A-173R-1, 100–101 cm: silica cement made of interconnected lepispheres. **b** Sample 313-29A-164R-2, 86–88 cm: silicate cement made of isolated silica lepispheres cemented by fibrous K-silicate (illite). **c** Sample 313-28A-40-1, 76–80 cm: tabular euhedral gypsum crystals covering a detrital quartz grain. **d** Sample 313-29A-173R-1, 100–101 cm: micronodule of jarosite cemented by microspheres and fibrous silica

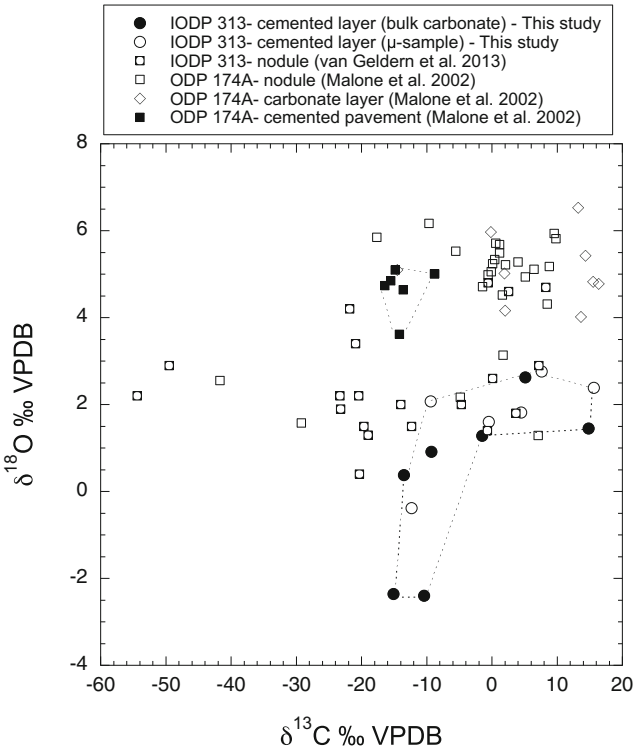

Fig. 7 Oxygen and carbon isotopic compositions of diagenetic carbonates of lithified layers from the IODP 313 drilling sites M0027A, M0028A and M0029A (from bulk powdered samples (*filled circle*) and micro-samples (*open circle*) of the cement). The isotopic values measured on the diagenetic carbonate nodules (*circle within square*) from the same IODP 313 drilling sites (van Geldern et al. 2013), and from the diagenetic carbonate nodules (*open square*), layers (*open rhomb*) and pavements (*filled square*) of the ODP 174A sites 1071 and 1072 (Malone et al. 2002) are reported for comparison

oxic conditions must have prevailed during and after this phase, as indicated by gypsum and jarosite precipitation. The succession of geochemical reactions that occurred at various depths and different times during diagenesis of the New Jersey shelf sediments may thus be described as follows.

– Organic matter oxidation and bacterial sulphate reduction (BSR). This reaction occurs under anoxic conditions below the seafloor where dissolved sulphate is provided by diffusion from the overlying seawater:

$$2\,CH_2O + SO_4^{2-} \rightarrow H_2S + 2\,HCO_3^- \quad (1)$$

– Microbial anaerobic oxidation of methane (AOM) coupled with reduction of sulphate. This reaction occurs in the sulphate–methane transition zone (SMTZ), where the downward flux of sulphate reacts with the upward flux of methane:

$$CH_4 + SO_4^{2-} \rightarrow HS^- + HCO_3^- + H_2O \quad (2)$$

– Methanogenesis by acetate fermentation. This reaction is typically located below the SMTZ:

$$CH_3COO^- + H^+ \rightarrow CH_4 + CO_2 \quad (3)$$

– Carbonate precipitation (reaction 4) and pyrite precipitation (reaction 5). These reactions are promoted by the release of alkalinity and sulphide during reactions 1 and 2, and by the availability of cations in pore fluids:

$$\left(Ca^{2+}, Mg^{2+}, Fe^{2+}\right) + 2\,HCO_3^- \rightarrow (Ca, Mg, Fe)\,CO_3 + CO_2 + H_2O \quad (4)$$

$$Fe^{2+} + 2\,HS^- \rightarrow FeS_2 + H_2 \quad (5)$$

– Carbonate and silicate chemical weathering with CO_2 produced during methanogenesis (reaction 3). These reactions lead to carbonate dissolution (reaction 6), silica and illite/glauconite precipitation (reaction 7) and carbonate precipitation (reaction 8):

$$(Ca, Mg, Fe)\,CO_3 + CO_2 + H_2O \rightarrow \left(Ca^{2+}, Mg^{2+}, Fe^{2+}\right) + 2\,HCO_3^- \quad (6)$$

$$(K, Mg, Fe)\ \text{silicates} + CO_2 + H_2O \rightarrow \text{illite/glauconite} + \left(K^+/Mg^{2+}/Fe^{2+}\right) + \text{silica} + HCO_3^- \quad (7)$$

$$\left(Ca^{2+}, Mg^{2+}, Fe^{2+}\right) + 2\,HCO_3^- \rightarrow (Ca, Mg, Fe)\,CO_3 + CO_2 + H_2O \quad (8)$$

– Pyrite oxidation (reaction 9), carbonate dissolution and gypsum precipitation (reaction 10), jarosite and silica precipitation (reaction 11):

$$FeS_2 + 2\,O_2 + 4\,H_2O \rightarrow Fe^{3+} + 2\,H_2SO_4 + 3\,e^- \quad (9)$$

$$CaCO_3 + H_2SO_4 \rightarrow CaSO_4,\ 2\,H_2O + CO_2 \quad (10)$$

$$\text{K–Fe silicates} + H_2SO_4 \rightarrow KFe_3(SO_4)_2(OH)_6 + \text{silica} \quad (11)$$

Reactions 1 to 8 take place under reducing conditions, whereas the subsequent reactions 9 to 11 occur under oxidizing conditions to produce the paragenetic sequence of authigenic minerals observed in the cements of lithified layers. It is important to note that there are different reactions leading to the precipitation and dissolution of carbonates and silicates, depending on the alkalinity and dissolved CO_2 concentrations,

as well as on the sulphur redox state in the pore solutions. These reactions would have been maintained at steady state conditions during enough time to control the rate and extent of mineralogical transformations after the deposition of New Jersey shelf sediments.

Characterization of diagenetic fluids

The oxygen isotopic composition of a carbonate depends both on the temperature and on the oxygen isotopic composition of the water during carbonate precipitation, assuming that such precipitation occurred at chemical and isotopic equilibrium. The equations relating these parameters for calcite (Kim and O'Neil 1997), dolomite (Fritz and Smith 1970) and siderite (Carothers et al. 1988) were used to define the theoretical $\delta^{18}O$ values of these carbonates at equilibrium for the local environmental conditions. At the present day, the temperature of bottom seawater on the shelf varies seasonally in the range 5–15 °C with an average value of 10 °C (van Geldern et al. 2013); the geothermal gradient has been estimated to be 40 °C/km (Mountain et al. 1994).

The studied samples of cemented layers at sites M0027A and M0029A are surrounded by pore waters with $\delta^{18}Ow$ of ca. –5‰ and ca. –1‰ respectively (Fig. 3; van Geldern et al. 2013). The estimations of the temperature of precipitation of carbonate cements in isotopic equilibrium with in situ pore waters at present-day depths give very low values (1 to 7 °C) at site M0027A and higher values (14 to 22 °C) at site M0029A (Table 3). These temperature estimates are lower than the theoretical temperatures at the present-day burial depth, which would range from 23±5 to 37±5 °C for a geothermal gradient of 40 °C/km (Table 3). This indicates that the carbonate cements were not precipitated in isotopic equilibrium for the present-day local conditions of burial depth, but at smaller burial depth. Moreover, the best estimates of temperature would range from 14 to 22 °C for pore water $\delta^{18}O$ values ranging from −3‰ to −1‰ (Table 3). Such $\delta^{18}O$ values of water would correspond to mixtures of seawater with a variable contribution of meteoric water. This interpretation is well consistent with the context of submarine groundwater discharge that characterizes the New Jersey continental shelf (Cohen et al. 2010; Skarke et al. 2014). The diagenetic carbonate nodules, layers and pavements collected from the same IODP sites M0027A, M0028A and M0029A (van Geldern et al. 2013) and from ODP Leg 174A sites 1071 and 1072 (Malone et al. 2002) exhibit much higher $\delta^{18}O$ values (+0.4 to +4.8‰ on the upper shelf and +1.6 to +6.5‰ on the outer shelf) than the carbonate cement of the lithified layers analyzed in this study (Fig. 6). The abovementioned authors underlined that the diagenetic carbonates were precipitated out of isotopic equilibrium with the present-day pore fluids; they concluded that diagenetic carbonate precipitation occurred in marine pore fluids either at cooler temperature than today and/or in seawater with higher $\delta^{18}O$ values than today.

Table 3 Calculated temperature of precipitation of carbonate cements of lithified layers sampled at sites M0027A, M0028A and M0029A

Sample (depth mbsf)	$\delta^{18}O$ ‰ VPDB	In situ T (°C)	In situ δw ‰ VSMOW	T (°C) equilibrium with in situ δw	T (°C) calcite (δw=−7)	T (°C) dolomite (δw=−7)	T (°C) siderite (δw=−7)	T (°C) calcite (δw=−3)	T (°C) dolomite (δw=−3)	T (°C) siderite (δw=−3)	T (°C) calcite (δw=−1)	T (°C) dolomite (δw=−1)	T (°C) siderite (δw=−1)
313-27A-171-1-38, 39 cm (489.8 mbsf)	2.8	30	−5	1			−5			8			15
313-27A-174-1-75, 76 cm (494.5 mbsf)	1.8	30	−5	4			−2			11			18
313-27A-190-1-31, 33 cm (533.7 mbsf)	−2.4	31	−5	7	−6			13			20		
313-28A-40-1-76, 80 cm (327.6 mbsf)	2.1	23	No data				−3			10			17
313-28A-123-1-67, 69 cm (540.0 mbsf)	−0.4	32	No data			1			18			28	
313-28A-169-2-14, 15 cm (664.0 mbsf)	−2.8	37	No data		−6			13			20		
313-29A-72-1-26, 28 cm (343.6 mbsf)	1.6	24	−1	16		−6			10			16	
313-29A-119-1-2, 4 cm (479.5 mbsf)	2.4	29	−1	14		−10			6			14	
313-29A-164-2-86, 88 cm (611.9 mbsf)	−2.4	36	−1	22	−6			13			22		

The $\delta^{13}C$ signatures of DIC ($\delta^{13}C_{DIC}$) of pore waters measured at the three sites M0027A, M0028A and M0029A (Fig. 8) display generally negative values (down to −13.1‰) with a few positive excursions (up to +7.2‰; van Geldern et al. 2013). Owing to the carbon enrichment factor ($\varepsilon^{13}C_{carbonate\text{-}DIC} = \delta^{13}C_{carbonate} - \delta^{13}C_{DIC}$) between DIC (i.e. mostly HCO_3^- in seawater) and carbonate, which is around +0.6‰ and +2.9‰ at 18 °C (the average estimated temperature of carbonate precipitation) for calcite and dolomite respectively (Rubinson and Clayton 1969; Sheppard and Schwarcz 1970), the $\delta^{13}C$ values of the carbonate cements precipitated in isotopic equilibrium with the present-day DIC would range between −4.3‰ and +1.9‰. In fact, the $\delta^{13}C$ values measured in the diagenetic cements are either lower or higher than these equilibrium values, meaning that the carbonates of the cements were not precipitated with the present-day pore fluid DIC (Fig. 8), thus confirming the conclusion based on the oxygen isotopic composition of carbonates. Conversely, the $\delta^{13}C_{DIC}$ values of pore fluids at the time of carbonate cementation (calculated from the carbon enrichment factor equation for calcite or dolomite) would range between −16.4‰ and +11.9‰. This indicates that the $\delta^{13}C$ values of the carbonate cements are related to organic matter diagenesis, which provided ^{13}C-depleted DIC during bacterial sulphate reduction and anaerobic oxidation of methane, and ^{13}C-rich DIC during methanogenesis by acetate fermentation (Claypool and Threlkeld 1983; Whiticar 1999).

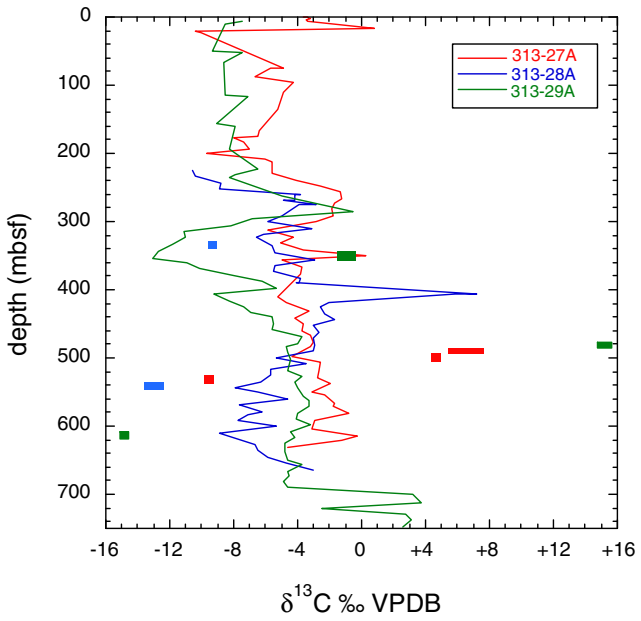

Fig. 8 Comparison of the depth distribution of $\delta^{13}C$ values of carbonate cement from lithified layers and of present-day pore water DIC at the IODP drilling sites M0027A, M0028A and M0029A (DIC data from van Geldern et al. 2013)

To summarize, multistep biogeochemical reactions controlled the precipitation of authigenic minerals in the indurated layers of the New Jersey upper continental shelf, by increasing DIC, cations and silica concentrations in the pore fluids, either under anoxic conditions as indicated by the carbon isotopic composition of the authigenic carbonates and the occurrence of pyrite, or under oxic conditions during later stages of diagenesis leading to the precipitation of sulphate minerals and to carbonate dissolution. Moreover, the depth distribution of the oxygen and carbon isotopic compositions of the carbonate cements shows that these carbonates are not in isotopic equilibrium with the present-day pore fluids. This means that carbonate precipitation of the cements occurred during past events where the depth distribution of the diagenetic zones was different from the present-day one. Opal-CT represents the late diagenetic cement of the lithified layers lying below 490 mbsf, where the in situ temperatures are estimated between 30 and 37 °C (Table 3). This range of temperatures fits well with the temperature estimates (18–56 °C) proposed for the formation and stability of opal-CT in the Monterey Formation (Keller and Isaacs 1985). It is thus inferred that silica cementation in the sediments of the New Jersey upper continental shelf occurred at burial depths close to the present-day ones, meaning that it represents a relatively recent diagenesis.

Conclusions

The New Jersey margin represents a case study of shallow shelf marine settings where siliciclastic sedimentation registered global sea-level variations and climate changes during the late Cenozoic. The diagenetic processes leading to cementation of these siliciclastic deposits of the upper continental shelf included organic matter diagenesis and chemical weathering of reactive silicate minerals by CO_2-rich pore waters issued from sulphate reduction, anaerobic oxidation of methane and methanogenesis. These reactions released bicarbonate, cations and dissolved silica in the pore fluids, which were further precipitated as carbonate, opal-CT and clay mineral cements. The temperature range (18±4 °C) estimated for the precipitation of the carbonate cements indicates that this cementation occurred at moderate burial depths, i.e. probably soon after deposition of these sediments during the early to middle Miocene. The later stage of silicate cementation is thought to have occurred at deeper burial depths, and characterizes recent diagenesis. In the specific context of the New Jersey margin, the submarine groundwater circulation of fresh water and the mixing with marine water at the boundaries between these two fluids of different chemistries played a significant role in the cementation process, especially by increasing the rate and intensity of chemical weathering of silicate minerals.

Acknowledgements This research used samples and data provided by the Integrated Ocean Drilling Program (IODP) and the International Continental Scientific Drilling Program (ICDP). The authors would like to thank Gerald Dickens for his very constructive review comments, which helped improve the article.

Compliance with ethical standards

Conflict of interest The authors declare that there is no conflict of interest with third parties.

References

Austin JA Jr, Christie-Blick N, Malone MJ et al (1998) Proc ODP, Init Repts 174A. Ocean Drilling Program, College Station, TX. doi:10.2973/odp.proc.ir.174a.1998

Burnett WC, Bokuniewicz H, Huettel M, Moore WS, Taniguchi M (2003) Groundwater and pore water inputs to the coastal zone. Biogeochemistry 66:3–33

Carothers WW, Adami LH, Rosenbauer RJ (1988) Experimental oxygen isotope fractionation between siderite-water and phosphoric acid-liberated CO_2-siderite. Geochim Cosmochim Acta 33:49–64

Christie-Blick N, Austin JA Jr, Shipboard Scientific Party (1998) Introduction: Oligocene to pleistocene eustatic change at the New Jersey continental margin. A test of sequence stratigraphy. In: Austin JA Jr, Christie-Blick N, Malone MJ et al., Proceedings of the Ocean Drilling Program Initial Reports 174A:5–16

Claypool GE, Threlkeld CN (1983) Anoxic diagenesis and methane generation in sediments of the Blake outer ridge, deep sea drilling project site 533, leg 76. In: Sheridan RE, Gradstein FM et al (eds) Init Repts DSDP 76. US Govt Printing Office, Washington, pp 391–402

Cohen D, Person M, Wang P, Gable CW, Hutchinson D, Marksamer A, Dugan B, Kooi H, Groen K, Lizarralde D, Evans RL, Day-Lewis FD, Lane JW Jr (2010) Origin and extent of fresh paleowaters on the Atlantic continental shelf, USA. Groundwater 48(1):143–158

Craig H (1957) Isotopic standards for carbon and oxygen and correction factors for mass-spectrometric analysis of carbon dioxide. Geochim Cosmochim Acta 12:133–149

Flörke OW, Hollmann R, von Rad U, Rösch H (1976) Intergrowth and twinning in opal-CT lepispheres. Contrib Mineral Petrol 58:235–242

Fritz P, Smith DGW (1970) The isotopic composition of secondary dolomites. Geochim Cosmochim Acta 34:1161–1173

Gonfiantini R, Stichler W, Kozanski K (1995) Standards and intercomparison materials distributed by the international atomic energy agency for stable isotope measurements. In: Reference and Intercomparison materials for stable isotopes of light elements, IAEA-TECDOC-825. IAEA, Vienna, pp 13–29

Hathaway JC, Poag CW, Valentine PC, Miller RE, Schultz DM, Manheim FT, Kohout FA, Bothner MH, Sangrey DA (1979) US geological survey core drilling on the Atlantic shelf. Science 206(4418):515–527. doi:10.1126/science.206.4418.515

Inwood J, Lofi J, Davies S, Basile C, Bjerum C, Mountain G, Proust JN, Otsuka H, Valppu H (2013) Statistical classification of log response as an indicator of facies variation during changes in sea level: integrated ocean drilling program expedition 313. Geosphere 9(4): 1025–1043. doi:10.1130/GES00913.1

Kastner M (1979) Silica polymorphs. In: marine minerals. Reviews in mineralogy, vol 6. Mineralogical Society of America, pp 99–109

Keller MA, Isaacs CM (1985) An evaluation of temperature scales for silica diagenesis in diatomaceous sequences including a new approach bases on the Miocene Monterey formation, California. Geo-Mar Lett 5:31–35

Kim ST, O'Neil JR (1997) Equilibrium and non-equilibrium oxygen isotope effects in synthetic carbonates. Geochim Cosmochim Acta 61(16):3461–3475

Lofi J, Inwood J, Proust JN, Monteverde DH, Loggia D, Basile C, Otsuka T, Stadler S, Mottl MJ, Fehr A, Pezard PA (2013) Fresh-water and salt-water distribution in passive margin sediments: insights from integrated ocean drilling program expedition 313 on the New Jersey margin. Geosphere 9(4):1009–1024. doi:10.1130/GES00855.1

Malone MJ, Claypool G, Martin JB, Dickens GR (2002) Variable methane fluxes in shallow marine systems over geologic time. The composition and origin of pore waters and authigenic carbonates on the New Jersey shelf. Mar Geol 189:175–196

Miller KG, Snyder SW (eds) (1997) Proc ODP, Sci Results 150X. Ocean Drilling Program, College Station, TX. doi:10.2973/odp.proc.sr.150X.1997

Miller KG et al (1994) Proc ODP, Init Repts 150X. Ocean Drilling Program, College Station, TX. doi:10.2973/odp.proc.ir.150X.1994

Moore WS (1999) The subterranean estuary: a reaction zone of ground water and sea water. Mar Chem 65:111–125

Mountain GS, Miller KG, Blum P et al (1994) Proc ODP, Init Repts 150. Ocean Drilling Program, College Station, TX. doi:10.2973/odp.proc.ir.150.1994

Mountain GS, Proust JN, McInroy D, Cotterill C, the Expedition 313 Scientists (2010) Proceedings of the Integrated Ocean drilling Program, vol 313. Integrated Ocean Drilling Program Management International, Tokyo. doi:10.2204/iodp.proc.313.2010

Post VEA, Groen J, Kooi H, Person M, Ge S, Edmunds WM (2013) Offshore fresh groundwater reserves as a global phenomenon. Nature 504:71–78. doi:10.1038/nature12858

Rubinson M, Clayton RN (1969) Carbon 13 fractionation between aragonite and calcite. Geochim Cosmochim Acta 33:997–1022

Sheppard SMF, Schwarcz HP (1970) Fractionation of carbon and oxygen isotopes and magnesium between coexisting metamorphic calcite and dolomite. Contrib Mineral Petrol 26:161–198

Skarke A, Ruppel C, Kodis M, Brothers D, Lobecker E (2014) Widespread methane leakage from the sea floor on the northern US Atlantic margin. Nat Geosci 7:657–661. doi:10.1038/NGEO2232

van Geldern R, Hayashi T, Böttcher ME, Mottl MJ, Barth JAC, Stadler S (2013) Stable isotope geochemistry of pore waters and marine sediments from the New Jersey shelf: methane formation and fluid origin. Geosphere 9(1):96–112. doi:10.1130/GES00859.1

Whiticar MJ (1999) Carbon and hydrogen isotope systematics of bacterial formation and oxidation of methane. Chem Geol 161:291–314